Heliyon 10 (2024) e38635

Contents lists available at ScienceDirect

Heliyon

journal homepage: www.cell.com/heliyon

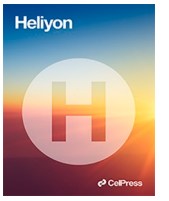

Research article

Exploring the mechanism of chondroitin sulfate-selenium nanoparticles in improving Alzheimer's disease: Insights from intestinal flora evaluation

Changfang Fu [a,b,1], Xinyue Wang [a,1], Wei Zhou [a,c], Qi Gao [a,d], Junjun Luo [a], Yuqin Li [a,*]

[a] School of Pharmaceutical Sciences & Institute of Materia Medica, Shandong First Medical University & Shandong Academy of Medical Sciences, Jinan, 250117, China
[b] Taishan vocational college of nursing, Taian 271000, China
[c] Heze Health School in Shandong Province, Heze 274000, China
[d] Key Laboratory of Clinical Pharmacology, Liao cheng People's Hospital, Liaocheng 252000, China

ARTICLE INFO

Keywords:
Alzheimer's disease
Chondroitin sulfate-selenium nanoparticles
Pathological section
Intestinal flora

ABSTRACT

In this study we have investigated the effect of chondroitin sulfate-selenium nanoparticles (CS@Se) on Alzheimer's disease (AD) mice using 16S rDNA technique. We randomly divided 30 SPF grade male C57BL/6 J mice into 6 groups according to random number table method. The AD mouse model was established by subcutaneous injection of D-galactose (D-gal) combined with gavage of $AlCl_3$ for 30 consecutive days, and then drug intervention was performed in the administration group for 40 consecutive days. The findings demonstrated several positive effects of CS@Se on AD mice. Firstly, CS@Se improved spatial learning and memory problems and reduces anxiety in AD mice. It also significantly reduced pyramidal cell arrangement disorder and rupture, leading to an improvement in synaptic structure damage between hippocampal neurons. Furthermore, CS@Se reduced mitochondrial swelling and vacuolation while increasing neuron survival in AD mice. Moreover, CS@Se significantly impacted the diversity and richness of intestinal flora in AD mice. It increased the relative abundance of Firmicutes and Actinobacteria while reducing the relative abundance of Bacteroidetes and Proteobacteria. In conclusion, CS@Se effectively reduced the breakdown of hippocampal pyramidal cells, improved the superfiber structure of hippocampal neurons, and restored intestinal flora balance, ultimately contributing to improving learning and memory abilities and alleviating anxiety in AD mice.

1. Introduction

Alzheimer's disease (AD), also known as senile dementia, is responsible for 50 %–60 % of dementia cases. It is a degenerative disease of the central nervous system characterized by a progressive and irreversible decline in memory, cognition, and executive function [1]. AD patients exhibit distinct pathological features in memory-related brain regions, including the formation of

* Corresponding author. School of Pharmaceutical Sciences & Institute of Materia Medica, Shandong First Medical University & Shandong Academy of Medical Sciences, Jinan, 250117, Shandong, China.
E-mail addresses: fuchangfang@126.com (C. Fu), liyuqin@sdfmu.edu.cn (Y. Li).
[1] *These authors have contributed equally to this work.*

https://doi.org/10.1016/j.heliyon.2024.e38635
Received 18 March 2024; Received in revised form 13 September 2024; Accepted 26 September 2024
Available online 28 September 2024

extracellular amyloid β-protein (Aβ) deposits known as age spots, intracellular neurofibrillary tangles caused by Tau protein hyperphosphorylation, and neuron loss [2,3]. Despite more than a century of research, the underlying causes of AD remain unclear. Several theories have been proposed, including gene mutation theory, Aβ toxicity theory, Tau abnormal modification theory, oxidative stress theory, inflammation theory, cholinergic injury theory, and neurovascular theory [4,5]. The World Alzheimer's Disease Report 2015 predicts that the number of dementia patients worldwide will reach 74.7 million by 2030 and 131.5 million by 2050, doubling approximately every 20 years [6], posing a significant threat to human health. However, more than 30 phase III clinical trials of drugs, including aducanumab approved by Food and Drug Administration (FDA), failed to achieve desirable results [7–9].

Chondroitin sulfate (CS) is primarily found in the cartilage and bones of mammals. CS possesses various physiological effects, including anti-arthritis [10,11], anti-oxidation [12,13], anti-coagulation and thrombosis [14], anti-atherosclerosis [15], antiviral [16] and anti-tumor properties [17], and the ability to regulate nerves [18]. Research has shown that CS can form an extracellular reticular structure around the neural fiber network, playing a crucial role in axon growth, synaptic plasticity, and the formation of glial scars [19]. In vitro cell experiments have demonstrated that low molecular weight chondroitin sulfate (LMWCS) can inhibit neurotoxic damage induced by $A\beta_{25\text{-}35}$, enhancing the resistance of PC12 and human neuroblastoma cells (SH-SY5Y) to toxic damage. Animal experiments have further shown that LMWCS can ameliorate oxidative imbalance in the hippocampus and cortex of AD mice induced by $A\beta_{1\text{-}40}$, improve cholinergic system functionality, increase acetylcholine (Ach) levels in the brain, and enhance learning and memory abilities in mice [20]. These findings strongly suggest that CS may inhibit endogenous glycosaminoglycan-induced Aβ formation and possess multiple effects, including antioxidant properties and mitigation of mitochondrial dysfunction. Therefore, CS holds potential as a multi-target drug for the treatment of AD.

Selenium, an essential trace element in the human body, plays a vital role in humans and animals [21] and possesses anti-tumor properties [22], heavy metal resistance, antiviral effects, and antioxidant capabilities. Studies have revealed that selenium deficiency leads to reduced phagocytic activity of neutrophils and increased expression of inflammatory markers [23], and chronic selenium deficiency can contribute to various brain diseases, including Alzheimer's disease (AD). Selenium can regulate the levels of glutathione peroxidase (GPX) and thioredoxin reductase (TrxR) in the body, thereby promoting tissue cell antioxidation, anti-aging effects, and playing a crucial role in reducing oxidative stress in the brain [24]. These characteristics indicate that selenium has a positive impact on the treatment and prevention of AD. Additionally, experiments have demonstrated that nano-selenium can scavenge free radicals, including superoxide anions and singlet oxygen. However, it should be noted that nano-selenium solutions tend to be unstable and prone to aggregation precipitation, which diminishes their antioxidant activity.

Further, both chondroitin sulfate and selenium have certain neuroprotective and antioxidant effects. A combination of the two can not only improve the dispersibility and stability of nano-selenium but can also enhance their anti-AD effects, giving chondroitin sulfate-selenium nanoparticles (CS@Se) a potential multi-target anti-AD effect. In addition, in vitro studies have demonstrated that CS@Se can inhibit Aβ aggregation, mitigate cytoskeleton damage, counteract oxidative stress, and inhibit Tau hyperphosphorylation, thereby playing a role in the treatment of AD [25].

Previously, it was believed that the central nervous system controlled the gastrointestinal tract. However, recent scientific findings have revealed a bidirectional communication system between the gut and the brain. The gut and brain communicate through various mechanisms, three of which have been extensively studied in recent years. They are the vagus nerve, neurotransmitters, and gut microbiota [26,27]. The World Health Organization's survey report indicates that 89 % of conditions such as Parkinson's disease, Alzheimer's disease, irritability and depression are associated with disruptions in the brain-gut axis. The adult intestine harbors over 10,000 species of microorganisms, with the total number reaching an astounding 10^{14}, making it akin to another organ within the human body [28]. The intestinal flora plays a crucial role in promoting the absorption of nutrients, synthesizing vitamins, promoting the development of the immune system, maintaining its normal function, and inhibiting the proliferation of pathogenic microorganisms [29].

Although studies have shown that CS@Se has certain ameliorative effects on AD, the mechanism of its action in intestinal flora has not yet been reported. Therefore, in this study, D-gal and $AlC1_3$ were used to construct an AD model, and the anxiety and learning and cognitive function of the mice were assessed through behavioral tests to detect potential improvements of CS@Se on AD, and to initiate a preliminary investigation on its mechanism based on pathological sections and intestinal flora changes.

2. Materials and methods

2.1. Materials

CS (Mw = 3.9 kDa) was provided by Prof. Xiao Yuliang's laboratory at Shandong First Medical University. CS@Se was prepared in our laboratory [24]. Sodium selenite (Na_2SeO_3) and L-cysteine (L-cys) were obtained from Aladd in Chemistry Co., Ltd. (Shanghai, China), D-(+) galactose and vitamin C were obtained from Beijing Solebo Technology Co., Ltd. (Beijing, China), aluminum trichloride was obtained from Tianjin Kaitong Chemical Reagent Co., LTD. (Tianjin, China), and saline injection was obtained from Chenxin Pharmaceutical Co., Ltd. (Jining, China). All other chemicals and reagents were of analytical purity grade.

2.2. Animals and housing

SPF-grade male C57BL/6 J mice (age: 8 weeks old, weight: 18–22 g) were purchased from Henan Skbex Biotechnology Co., Ltd. They were kept at a temperature of 23–25 °C, humidity of 45–55 %, a 12-h light/dark cycle, and provided ad libitum access to food and water. All animal experiments were conducted in accordance with the guidelines set by the Institutional Animal Ethics Committee and

were approved by the Experimental Animal Ethics Committee of Shandong First Medical University (No.: W202302200002).

After one week of acclimatization, the mice were weighed and randomly divided into six groups, each consisting of 5 mice. The groups were as follows: the control group, model group, vitamin C group (VC group), CS@Se low-dose group (L-CS@Se group), CS@Se medium-dose group (M-CS@Se group), and CS@Se high-dose group (H-CS@Se group). In the first 30 days, the following steps were performed. The control group received both gavage and subcutaneous injections of normal saline (10 mL/kg·d), while the other five groups received gavage administration of $AlCl_3$ (100 mg/kg·d) and subcutaneous injections of D-gal (60 mg/kg·d) to induce the AD in the mice. Once the AD model was established, the following administrations were carried out: the control group and model group received gavage administration of double steamed water (10 mL/kg·d), the VC group received gavage administration of vitamin C (65 mg/kg·d), the CS@Se low-dose, medium-dose and high-dose groups received gavage administration of CS@Se (50 mg/kg·d, 100 mg/kg·d, 200 mg/kg·d) for 40 consecutive days, with the modeling process continued during the administration period. Behavioral tests were conducted 24 h after the final administration and continued until the end of the study.

2.3. Behavioral tests

2.3.1. Morris water maze (MWM)

The MWM, developed by British psychologist Richard G. Morris in 1981, is a widely used method for assessing spatial learning [30,31]. The experimental setup consists of a circular pool, a platform, a camera system, and an analysis system (the Tianmin USB Box series application and Tracking Master V3.0). The pool is divided into four quadrants, and a transparent platform is placed in the fourth quadrant. The pool is filled with clear water, with the water level maintained 1 cm above the platform.

The MWM experiment consists of two parts: the positioning navigation experiment and the spatial exploration experiment, which assess the spatial positioning ability and learning and memory abilities of the mice, respectively. In the positioning navigation experiment, the mice were placed into the water from each of the four quadrants, with their heads facing the pool wall. They were given 60 s to locate the platform. The objective was for the mice to memorize the platform's position and successfully climb onto it during the multiple days of continuous training. If a mouse found the platform within 60 s, the computer automatically recorded the time taken to reach the platform, known as the escape latency, and the mouse was allowed to rest on the platform for 10 s. In cases where a mouse failed to find the platform within the allocated time, it was guided to the platform and encouraged to remain on it for 20 s to enhance learning and memory. At the end of each experiment, the mice were removed from the water, dried, and returned to their cages. Twenty-four hours after the completion of the positioning navigation experiment, the platform in the fourth quadrant was removed. The mice were then placed into the water from the second quadrant using the same method as in the positioning navigation experiment. Within a 60-s timeframe, the movement tracks, number of platform crossings, and time spent in the target quadrant (fourth quadrant) were recorded for each mouse.

2.3.2. Novel object recognition test (NOR)

The NOR experiment is a behavioral test that assesses the memory recognition capabilities of mice by exploiting their natural inclination to approach and explore new objects. The experimental setup involves an open field activity box, objects labeled as A_1, A_2 and B, a camera system, and video analysis software (the Tracking Master V3.0) designed for data processing and analysis.

The first day of the NOR experiment served as the adaptation stage. Each mouse was placed individually in an autonomous activity box without any objects and allowed to freely explore for 5 min. On the second day, memory training was conducted. Two objects, A_1 and A_2, made of the same material and size, were positioned in the upper right corner and lower left corner of the autonomous activity box, respectively. The mice were placed in the box with their backs to the objects and were given 5 min to freely explore their surroundings. On the third day, object A_2 was replaced with a new object labeled as B. The mice were placed in the activity box using the same procedure as the second day, and the video recording was immediately initiated. The mice were allowed to move freely and explore for 5 min. The duration of time the mice spent touching objects A_1 and B (t_{A1}, t_B) was recorded, and the preference index (PI) of each mouse was calculated using the formula $PI = t_B/(t_{A1} + t_B)$. After each mouse's experiment, the autonomous activity box and objects were wiped with alcohol to remove any residual odor, and the next experiment was conducted once the alcohol had evaporated to prevent any interference from lingering scents.

2.3.3. Y maze

The Y maze is a commonly used apparatus to assess the learning and memory capabilities of mice by capitalizing on their natural inclination to explore new environments [32]. It consists of three identical closed arms, a camera recording system and a video analysis system (the Tracking Master V3.0). The three closed arms in the Y maze are of equal length and are numbered as No. 1, No. 2, and No. 3. The angle between each pair of closed arms is precisely 120°, forming a Y-shaped configuration.

During the Y maze test, the mice were placed in the central area of the maze and allowed to freely explore for 10 min. The camera system recorded the behavioral changes of the mice throughout the entire 10-min period. Each time a mouse entered a closed arm, the corresponding arm number was recorded, and the mice were expected to exhibit complete alternating behavior by sequentially entering each of the three closed arms. The number of complete alternations (n) and the total number of closed-arm entries (N) were recorded for each mouse. The spontaneous alternation ratio was calculated as the number of complete alternation times (n)/maximum alternations times (N-2) × 100 % (P = n/(N-2) × 100 %) [33,34]. At the end of each mouse's free exploration session in the maze, the experimental apparatus was required to be wiped with alcohol, and the next experiment was carried out after the alcohol was volatilized.

2.3.4. Passive avoidance test (PAT)

The PAT, also known as the light-dark box shuttle test, uses the natural aversion of mice to dark and aversive stimuli to assess their memory capabilities. The experimental setup consists of two boxes of identical size (a dark box with an electrifying device at the bottom, and a light box separated by a fence), which allows the mice to pass between them. The TopScan Version 3.0 was used in recording the PAT.

During the adaptation phase on the first day, the mice were placed in the light room with their backs facing the dark box and were allowed to move freely for 2 min. The next day, the mice were again placed in the light room using the same procedure as the previous day. Once the mice entered the dark box, the fence separating the boxes was closed, and the mice were subjected to three instances of a 0.4 A current for 10 s each. On the third day of the test period, the mice were again placed in the light room following the same procedure. The time it took for each mouse to enter the dark box for the first time, known as the escape latency, was recorded. After each mouse completed the test, the experimental apparatus was wiped with alcohol, and the next experiment was carried out after the alcohol was volatilized.

2.3.5. Open field test (OFT)

The OFT experiment is a widely used behavioral test designed to assess the exploratory and anxiety-related behaviors of mice in an unfamiliar environment [35]. The experimental setup typically consists of an open field experimental box, a video recording system, and an analysis system (the Tracking Master V3.0). The bottom of the open field experimental box is divided into 16 parts of equal area, and the camera is placed on the top of the box.

The whole process of the OFT experiment was carried out in a quiet environment. At the start of the experiment, the mice were placed into the open field box with their heads facing downwards and their backs towards the object. The video recording started immediately after the mice were introduced into the box, and the experiment lasted for 10 min. During the experimental period, the incubation time of entering the central square, the duration of activity in the central square and the number of entries into the central square were recorded. Before the next mouse experiment, the inner wall and the bottom of the box were wiped with alcohol, and the experiment was performed after the alcohol had volatilized to avoid the interference of residual odor in the experiment.

2.4. Samples collection and processing

After the behavioral test, the mice were euthanized by cervical dislocation, and their eyeballs were removed to collect blood samples. The mice were fixed in a supine position, and the abdominal and front thoracic walls were carefully incised to expose the internal organs. A sac, known as the cecum, was identified near the anus, and approximately 3 cm of colon tissue behind it was carefully collected and placed into sterilized centrifuge tubes. The tubes containing the colon tissue were then frozen at −80 °C for further analysis. Next, the intact brain tissues of the mice were immediately extracted and immersed in pre-cooled paraformaldehyde solution and electron microscope fixation solution, respectively. The brain tissues were left to fix in the paraformaldehyde solution at room temperature for a minimum of 24 h, while the electron microscope fixation solution was used to fix the brain tissues at a temperature of 4 °C for more than 24 h.

2.5. Pathological sections

2.5.1. Hematoxylin and eosin (HE) staining

The brain tissues were removed from the paraformaldehyde solution, dehydrated and waxed, embedded and sliced successively, stained using HE, observed under a microscope, and the images were collected for analysis.

2.5.2. Transmission electron microscope

The tissues soaked in the electron microscope fixation solution were taken out, fixed, dehydrated, permeated, embedded, polymerized, sliced and stained successively, and the images were assessed using transmission electron microscopy.

2.6. High-throughput sequencing of intestinal flora

Samples of the colon contents were sent to Shandong Kaiyi Gene Technology Co., Ltd. for sequencing. The total microbial DNA was extracted from the samples using a kit, and the quality of DNA extraction was assessed using 0.8 % agarose gel electrophoresis. The DNA was quantified using an ultraviolet spectrophotometer. To amplify the ribosomal DNA (rDNA), conserved region-specific primers were used in the polymerase chain reaction (PCR) amplification. The PCR products were examined using 2 % agarose gel electrophoresis, and the target fragments were extracted from the gel. Based on the preliminary quantification results from electrophoresis, the PCR products were further quantified using fluorescence. According to the fluorescence quantitative results, each sample was mixed in the appropriate proportion to meet the sequencing volume requirements. The Illumina TruSeq Nano DNA LT Library Prep Kit was used to prepare the sequencing library. After the library was inspected for quality and after passing the quality assessment, machine sequencing was performed.

2.7. Statistical analysis

The IBM SPSS Statistics 25 software was used to analyze the data through one-way analysis of variance (ANOVA) and *t*-test. All

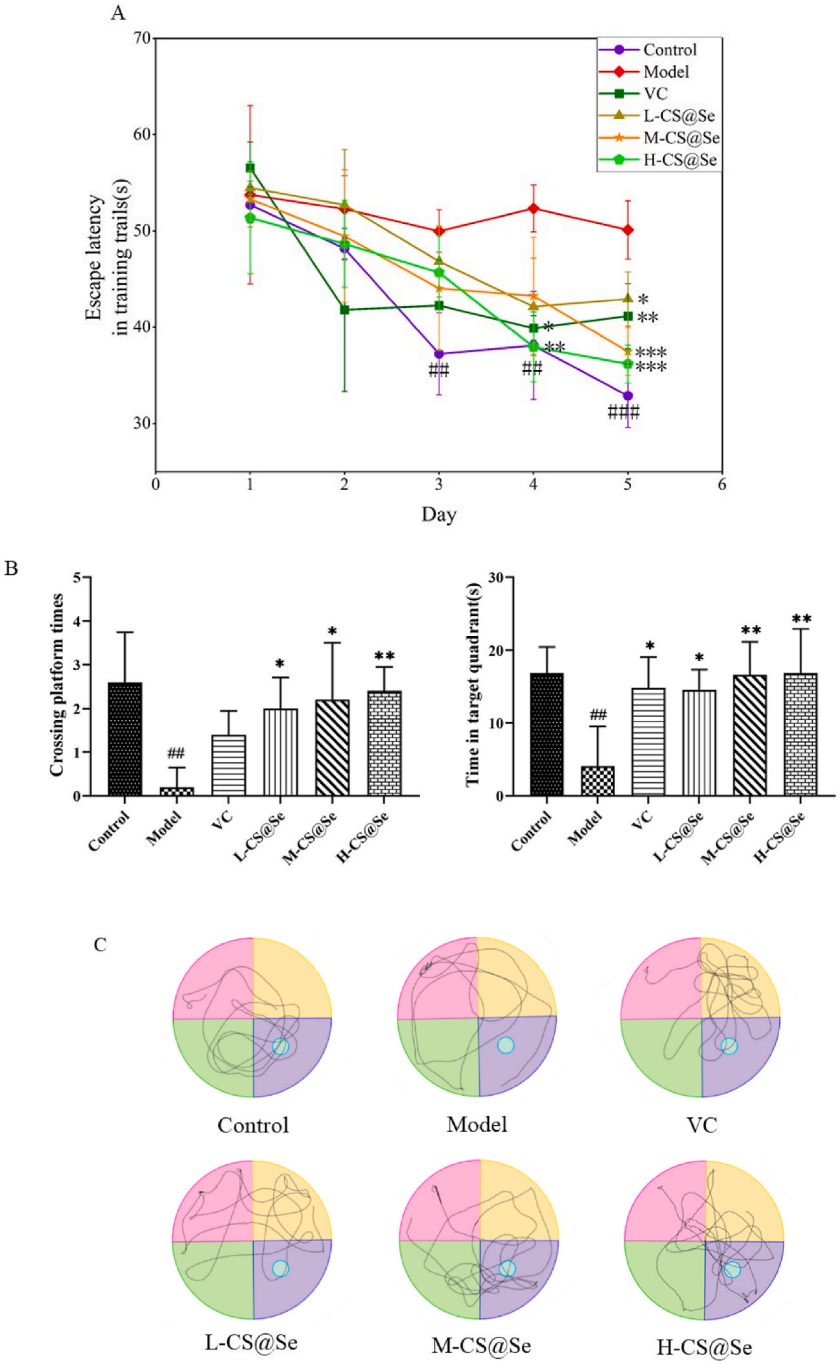

Fig. 1. Results of MWM (A, B, C), NOR (D), Y maze (E) and PAT (F).
Note: $^{\#}p < 0.05$, $^{\#\#}p < 0.01$, $^{\#\#\#}p < 0.001$ vs the control group; $^{*}p < 0.05$, $^{**}p < 0.01$, $^{***}p < 0.001$ vs the model group.

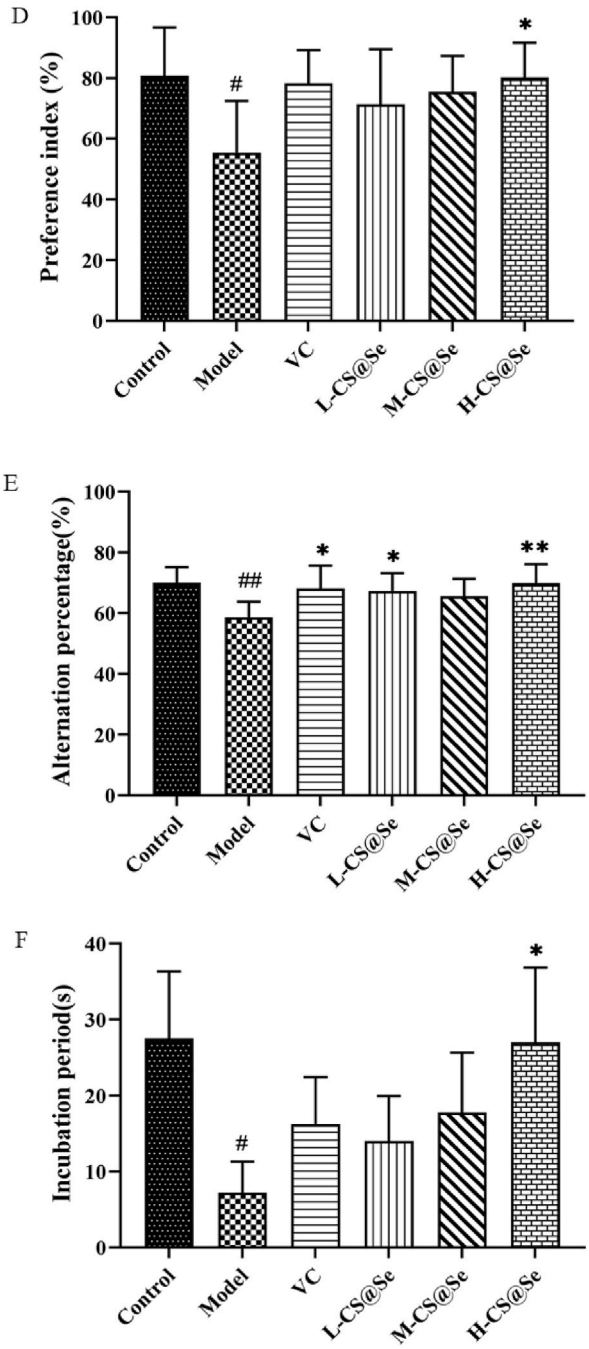

Fig. 1. (*continued*).

quantitative data were expressed as mean ± standard deviation. Differences in means with $p < 0.05$, $p < 0.01$ and $p < 0.001$ were considered to be significant, highly significant, and extremely significant, respectively.

3. Results

3.1. Results of behavioral experiments

3.1.1. Results of MWM, NOR, Y maze and PAT

Cognitive impairment is the earliest and most important clinical manifestation of AD. To investigate whether CS@Se can alleviate

the learning and memory impairment of AD mice induced by D-gal and $AlCl_3$, their spatial memory and learning memory were assessed using MWM, NOR, Y maze and PAT.

The results of the positioning navigation experiment in the Morris Water Maze (MWM) are presented in Fig. 1A. Compared to the control group, the mice in the model group exhibited a significant increase in escape latency starting from the third day ($p < 0.05$), indicating that D-gal and $AlCl_3$ induced spatial memory deficits in the mice. However, with increasing training time, the escape latencies of the VC group, L, M and H-CS@Se groups were significantly decreased compared to the model group ($p < 0.05$). These findings suggest that CS@Se treatment can effectively reduce escape latency and improve the spatial memory ability of AD mice. After 24 h of the positioning navigation experiment, the platform was removed to conduct the space exploration experiment (Fig. 1B and C). Compared to the control group, the model group exhibited a significant decrease in the number of platform crossings and the time spent in the target quadrant ($p < 0.01$). However, after 40 days of treatment, the VC group, L-CS@Se group, M-CS@Se group, and H-CS@Se group showed a significant increase in the number of platform crossings and residence time in the target quadrant compared to the model group ($p < 0.05$). These results indicate that CS@Se administration can ameliorate spatial memory impairments in AD mice induced by D-gal and $AlCl_3$.

NOR was performed to detect the recognition memory ability of the mice (Fig. 1D). Compared to the control group, the preference index for the new object in the model group was significantly decreased ($p < 0.05$), while the preference index in the H-CS@Se group was significantly higher than that in the model group ($p < 0.05$). These results suggested that high doses of CS@Se could improve the learning and memory of AD mice induced by D-gal and $AlCl_3$.

Y maze experiment results are shown in Fig. 1E. Compared with the control group, the model group exhibited a significant reduction in the spontaneous alternations ratio ($p < 0.01$), indicating that D-gal and $AlCl_3$ could cause significant short-term memory problems in mice. Compared with the model group, the spontaneous alternations ratios in VC, L-CS@Se and H-CS@Se groups were significantly increased ($p < 0.05$), while the spontaneous alternations ratio in the M-CS@Se group was increased, but the difference was not statistically significant. These results suggested that CS@Se could improve short-term memory problems in AD mice induced by D-gal and $AlCl_3$.

PAT was used to assess the memory ability of the mice (Fig. 1F). Compared to the control group, the incubation period of mice in the model group was significantly shortened ($p < 0.05$), indicating that AD mice had obvious memory problems. Compared with the model group, the incubation period of mice in the H-CS@Se group was significantly increased ($p < 0.05$), while the incubation periods of mice in the VC group, L-CS@Se group and M-CS@Se group were increased, but the difference was not statistically significant. These results suggested that high doses of CS@Se could improve memory problems in AD mice induced by D-gal and $AlCl_3$.

The results of MWM, NOR, Y maze and PAT showed that CS@Se could effectively improve the spatial memory and learning memory of AD mice.

3.1.2. Results of ORT

To investigate the potential effect of CS@Se on alleviating anxiety in AD mice induced by D-gal and $AlCl_3$, OFT was conducted (Fig. 2). The results showed that compared with the control group, the incubation period in the model group was significantly increased ($p < 0.01$), and the duration of stay in the center of the square and the number of entries in the center of the square was significantly reduced ($p < 0.01$), indicating that AD mice showed obvious anxious behavior. Further, compared with the model group, the incubation period of the VC group, M-CS@Se group and H-CS@Se group was significantly shorter ($p < 0.05$), the residence time of the VC group and H-CS@Se group in the center of the square was significantly increased ($p < 0.05$), and the times of entries to the center of the square in the M-CS@Se group and H-CS@Se group were significantly increased ($p < 0.05$). These results suggested that high doses of CS@Se could improve anxiety in AD mice induced by D-gal and $AlCl_3$.

3.2. Results of hippocampal histopathological section

3.2.1. Results of HE staining

The morphological changes of pyramidal cells in the CA1, CA3, and DG regions of the mice hippocampus were evaluated to assess

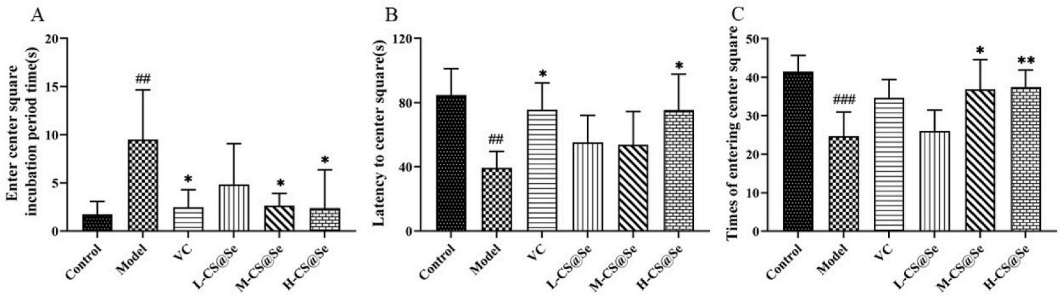

Fig. 2. Results of OFT
(Incubation period (A), Latency to center square (B), Times of entering center square (C))
Note: $^{\#\#}p < 0.01$, $^{\#\#\#}p < 0.001$ vs the control group; $^{*}p < 0.05$, $^{**}p < 0.01$ vs the model group.

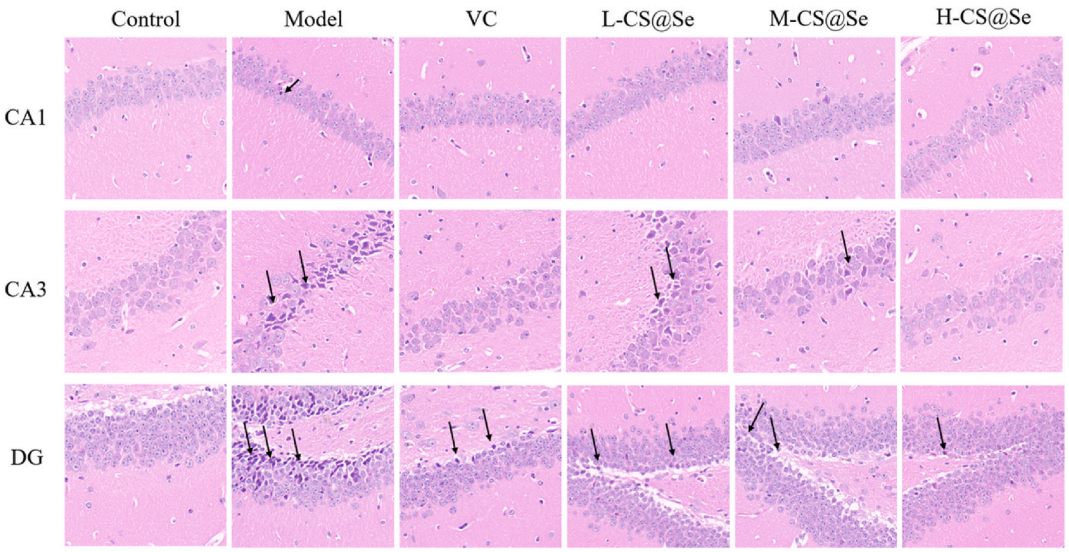

Fig. 3. Results of HE staining.

the extent of damage (Fig. 3). In the control group, the tissue structures of CA1, CA3 and DG regions in the hippocampus of the mice were clear, the pyramidal cells were neatly arranged and compact, the boundary was clear, the nuclei were large and round, with less chromatin, evident nucleoli, and no obvious abnormalities were observed. Compared to the control group, the arrangement of cells in the model group was disordered, and the number of cells was reduced. There were occasional pyramidal cell shrinkage and deep staining in the CA1 region and more pyramidal cell shrinkage and deep staining in CA3 and DG regions (black arrow in the figure). The boundary between the cytoplasm and the nucleus was not clear, and the cell shape was irregular. Compared with the model group, there was less damage to pyramidal cells in the VC group and the CS@Se low, medium and high dose groups, with clear tissue structures, regular arrangement of pyramidal cells, and occasional contraction and deep staining of pyramidal cells in CA3 and DG regions. Collectively, CS@Se and VC could improve the condition of hippocampal pyramidal cells in AD mice induced by D-gal and $AlCl_3$ to varying degrees, and as shown in the figure, the effects of the H-CS@Se group were more obvious.

3.2.2. Results of transmission electron microscope

The damages to the hippocampal tissues of mice were assessed by examining the synaptic and mitochondrial structures. Fig. 4 illustrates the synaptic and mitochondrial changes observed in the hippocampal tissues. Compared to the control group, the model group exhibited damaged synaptic structures in the hippocampus of mice. The postsynaptic dense zone was thinner, the relative surface was shorter, and the curvature of the synaptic curve was reduced (red arrow in the figure). Additionally, the mitochondria within the hippocampal neurons (green arrow in the figure) showed signs of swelling, reduced ridges and vacuoles (yellow arrow in the figure). Compared with the model group, the postsynaptic dense zone, relative surface of synapses and the curvature of the synaptic curve were improved in the VC group and the CS@Se low, medium and high dose groups. The mitochondrial ridges of hippocampal neurons were relatively intact, with reduced occurrence of vacuoles and mitochondrial swelling. These findings indicate that CS@Se could reduce mitochondrial apoptosis, improve the abnormal synaptic ultrastructure of hippocampal neurons in AD mice, and increase the survival of AD mice neurons.

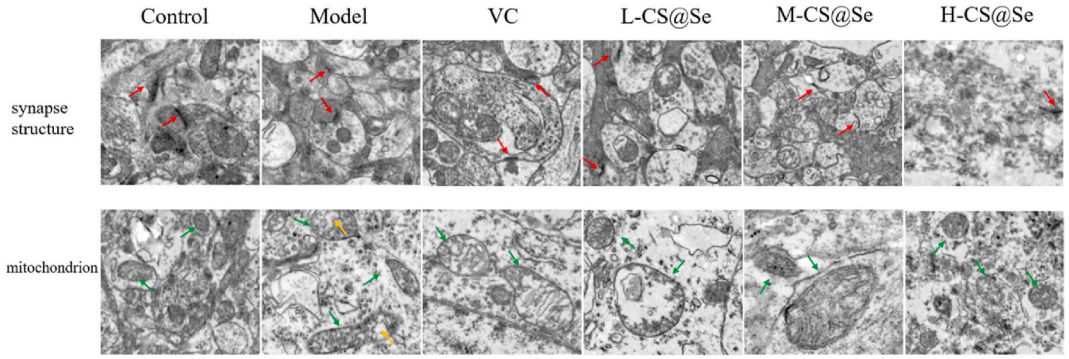

Fig. 4. Results of transmission electron microscope.

The HE staining and transmission electron microscope results showed that CS@Se could effectively reduce the breakdown and irregular arrangement of hippocampal pyramidal cells, improve the state of synapses and reduce mitochondrial apoptosis between neurons of AD mice induced by D-gal and $AlCl_3$.

3.3. Results of intestinal flora

3.3.1. Intestinal flora complexity

A total of 3,631,328 taxon tags were obtained from the 30 samples across six different processing groups to construct operational taxonomic units (OTUs), and species annotation information was obtained. The distribution of taxon tags in each group is presented in Table 1. On average, each sample contained 121,044 taxon tags. The highest number of taxon tags observed among all samples was 141,485, while the lowest number was 71,085.

Alpha diversity is a measure used to assess the microbial community diversity within a sample. It provides insights into the richness and evenness of the microbial species present within a single sample.

The species accumulation curve is valuable for examining the relationship between sample size and the number of observed species. It provides insights into species composition and helps predict species abundance in a given sample. This curve is widely used in biodiversity and community investigations to determine if the sample size is sufficient and estimate species richness. Therefore, the species accumulation curve can not only judge whether the sample size is sufficient but also predict the species richness under the premise that the sample size is sufficient. As shown in Fig. 5, the species accumulation curve gradually increased within a certain range as the sample size increased. This gentle slope suggests that the experiment achieved a thorough sampling, indicating that the sample size was adequate for data analysis.

The dilution curve, also known as the richness curve, is employed to assess whether the sequencing depth adequately captures species diversity in the samples to evaluate if the sequencing volume is sufficient to capture all taxa and indirectly reflects the species richness within the sample. As depicted in Fig. 6A, the curves for each sample exhibited a flattening trend as the sequencing volume increased, indicating that the amount of sequencing data used in this experiment was appropriate and that further increasing the data volume would only yield a few additional species. Moreover, there was no notable difference in the growth pattern of the dilution curve among the different groups, suggesting similar sequencing sufficiency across all groups.

Rank-abundance curves provide insights into species abundance and evenness within a community. As depicted in Fig. 6B, the width of the curve along the horizontal axis represents species richness, with a broader span indicating a higher species richness. In the vertical direction, the smoothness of the curve reflects the evenness of species distribution within the sample, with a gentler curve indicating a more even distribution of species.

The statistical analysis of the effective sequences included the calculation of various alpha diversity indexes, such as the Chao index, Ace index, Shannon index, Simpson index, and Goods coverage index. These indexes were compared to assess the differences in species richness and diversity of microbial communities among each sample. The results of the different alpha diversity indexes in each group were recorded in Table 2 and Fig. 7, and the magnitude of the index values reflected the complexity of the sample community.

The results showed that compared to the control group, the Ace index and Chao index of mice in the model group exhibited a decreasing trend, indicating a decrease in the richness of the intestinal flora in AD mice. Additionally, the Shannon index decreased while the Simpson index increased, indicating a decrease in intestinal flora diversity. Compared to the Model group, the administration of CS@Se effectively restored the above indexes in the CS@Se treatment groups, with the H-CS@Se group showing the best results. The Good's coverage index reflects sequencing depth, i.e., the coverage of the community, and the Good's coverage index of all six groups was higher than 0.99, indicating that the sequencing depth of this experiment has basically covered all species in the samples. It is worth noting that, possibly due to the complex and diverse of structure and composition of intestinal flora, the sample size of mice in each group was small and there were individual differences. Therefore, although CS@Se could significantly improve the richness and diversity of intestinal flora in AD mice, the differences were not statistically significant. This also suggests the need to expand the sample size for further exploration to elucidate the detailed mechanism of the effect of CS@Se on intestinal flora.

3.3.2. The distribution of intestinal flora

At the phylum level, bacteria with a relative abundance greater than 1 % are considered dominant. The results of the distribution of intestinal flora were recorded in Fig. 8. In the intestinal flora structure of mice in each group, Firmicutes, Bacteroidetes, and Proteobacteria were identified as the dominant phyla, collectively accounting for over 80 % of the total sequences. Compared to the control group, the model group exhibited decreased relative abundances of Firmicutes and Actinobacteria and increased relative

Table 1
The distribution of taxon tags in each group.

Groups	Total taxon tag	Average taxon tag	Taxon tag(min)	Taxon tag(max)
Control group	569024	113805	71085	130059
Model group	573796	114759	102320	129803
VC group	615926	123185	112156	132162
L-CS@Se group	635314	127063	116656	137441
M-CS@Se group	604787	120957	114830	129681
H-CS@Se group	632481	126496	115544	141485

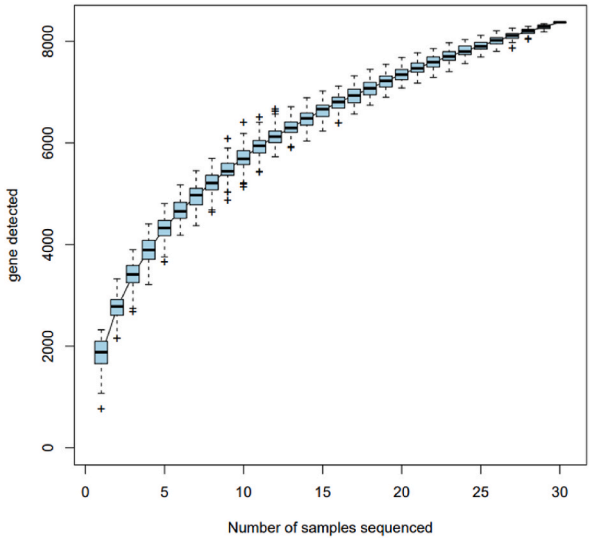

Fig. 5. Species accumulation curve.

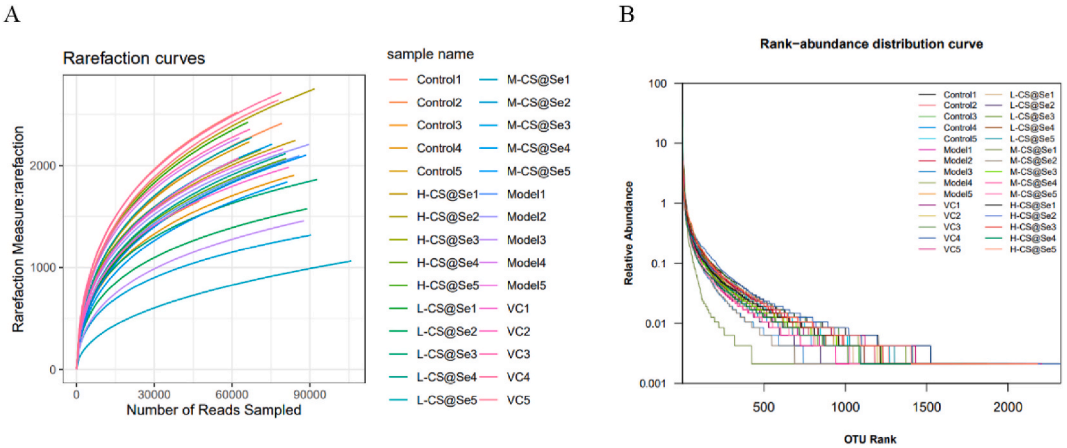

Fig. 6. Dilution curves of each sample (A) and rank-abundance curves of each sample (B).

Table 2
Statistical table of alpha diversity analysis index among groups.

Groups	Chao	Ace	Shannon	Simpson	Goods coverage
Control	3316 ± 144	3303 ± 157	7.78 ± 0.55	0.978 ± 0.003	0.990 ± 0.0020
Model	2662 ± 469	2625 ± 480	7.38 ± 0.82	0.984 ± 0.009	0.991 ± 0.0017
VC	3213 ± 384	3229 ± 417	7.85 ± 0.60	0.979 ± 0.011	0.990 ± 0.0019
L-CS@Se	2670 ± 420	2732 ± 414	7.15 ± 0.31	0.970 ± 0.012	0.992 ± 0.0024
M-CS@Se	2682 ± 577	2624 ± 552	6.81 ± 0.42	0.958 ± 0.010	0.993 ± 0.0024
H-CS@Se	3287 ± 383	3222 ± 363	7.64 ± 0.76	0.968 ± 0.038	0.990 ± 0.0015

abundances of Bacteroidetes and Proteobacteria. In contrast, the administration groups showed up-regulation of Firmicutes and Actinobacteria while down-regulating the abundances of Bacteroidetes and Proteobacteria compared to the model group.

At the class level, the model group exhibited lower relative abundances of Bacteroidia, Clostridia, and Desulfovibrionia than the control group. Conversely, the model group showed increased relative abundances of Verrucomicrobiae, Bacilli, Campylobacteria, Saccharimonadia, and Coriobacteriia. In contrast, the administration groups were able to up-regulate the relative abundances of Bacteroidia, Clostridia and Desulfovibrionia, while down-regulating the relative abundances of Verrucomicrobiae, Bacilli, and Campylobacteria compared to the model group.

At the order level, there were significant variations in the relative abundance of Lactobacillales, a probiotic group, among the

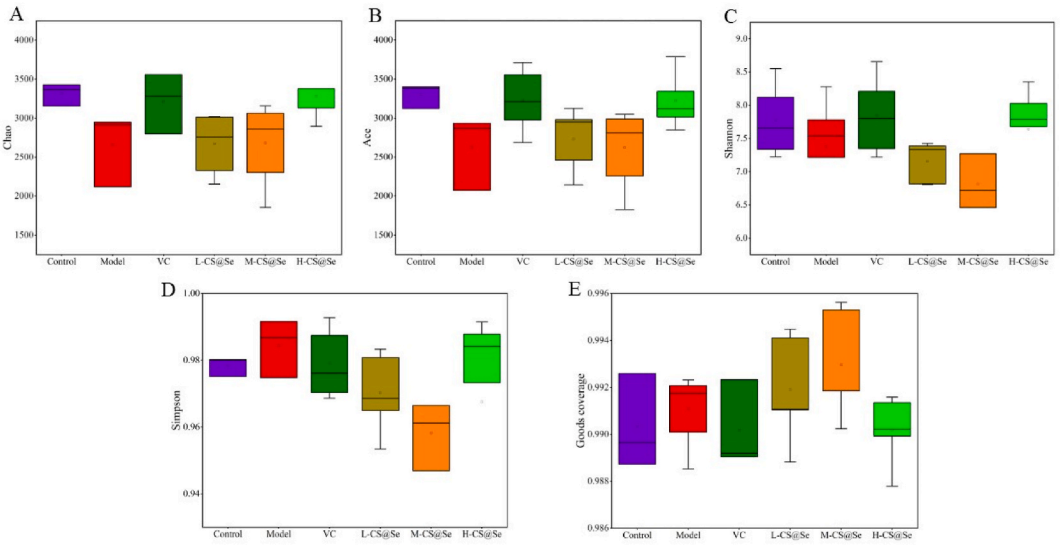

Fig. 7. Statistical graph of alpha diversity analysis index among groups
(Chao index (A), Ace index (B), Shannon index (C), Simpson index (D), Good's coverage index (E)).

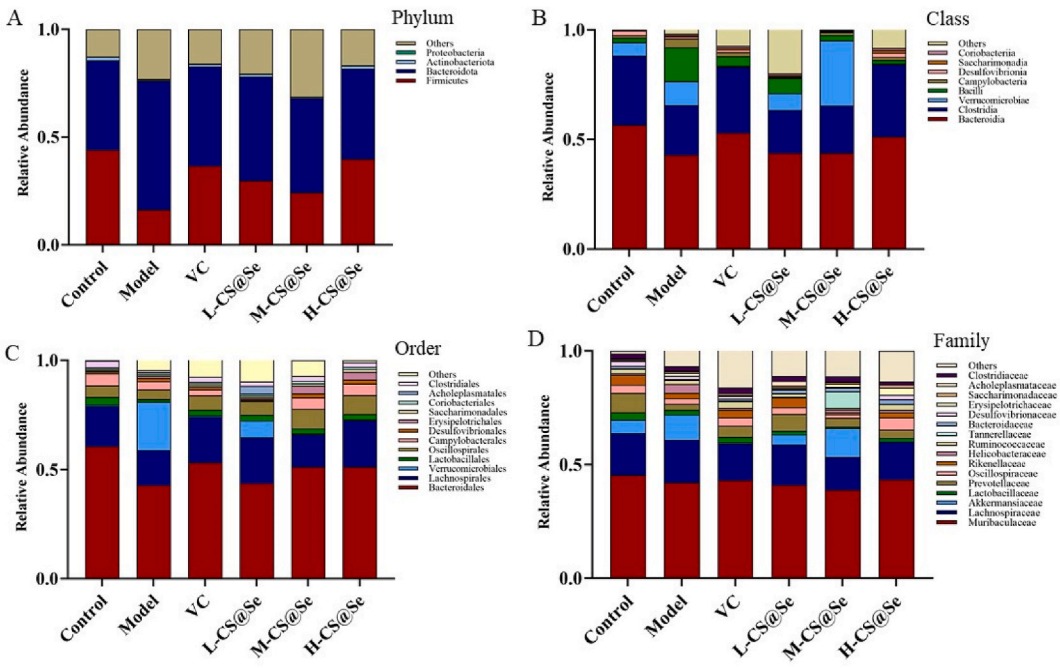

Fig. 8. Comparison of the relative abundance of flora at the four classification levels
(Phylum (A), Class (B), Order (C), Family (D)).

different groups. Compared to the control group (0.0342), the model group showed a nearly 2.6-fold reduction in the relative abundance of Lactobacillales (0.0131). After 40 days of administration, the relative abundance of Lactobacillales in each group increased compared to the model group. The VC group and L-CS@Se group showed the most pronounced effects, with relative abundances of 0.0258 and 0.0261, respectively. Furthermore, compared to the control group, the model group exhibited decreased relative abundances of Bacteroidales, Lachnospirales and Campylobacterales while showing increased relative abundances of Verrucomicrobiales and Erysipelotrichales. After treatment, the relative abundances of these corresponding bacteria were improved.

At the family level, the trend observed for Lactobacillaceae was consistent with that at the order level. The relative abundance of Lactobacillaceae decreased in AD mice induced by D-gal and $AlCl_3$ and improved after treatment. In the gut microbiota of mice in the model group, the relative abundance of Helicobacteraceae reached as high as 0.0386, which is 5.9 times higher than that in control

group normal mice (0.0068)! Additionally, Muribaculaceae and Lachnospiraceae were found to be dominant flora. However, the relative abundances of Muribaculaceae and Lachnospiraceae were not significantly different among the six groups. The highest relative abundance of Muribaculaceae was 0.4548 in the control group, while the lowest was 0.3905 in the M-CS@Se group. For Lachnospiraceae, the highest relative abundance was observed in the model group (0.1859), while the lowest was in the M-CS@Se group (0.1427).

Taken together, CS@Se administration improved the diversity and richness of intestinal flora in AD mice induced by D-gal and $AlCl_3$. It increased the relative abundance of Firmicutes and Actinobacteria while reducing the relative abundance of Bacteroidetes and Proteobacteria. Notably, CS@Se also significantly increased the relative abundance of Lactobacillaceae.

3.3.3. The composition of intestinal flora

According to the species annotation and abundance information at the phylum level, clustering analysis was performed based on species and samples, and heat maps were generated, which showed consistent patterns with the variations in the relative abundance of phylum level (Fig. 9). Compared to the control group, the model group exhibited higher concentrations of Bacteroidetes, Proteobacteria, Deinococcota, Chloroflexi, Spirochaetota and Myxococcota, while the levels of Firmicutes, Actinobacteriota, Cyanobacteria, Fibrobacterota and Desulfobacterota were lower. In the VC group, the concentrations of Chloroflexi, Acidobacteriota, Firmicutes, Actinobacteriota, Cyanobacteria and Deferribacterota were relatively higher, while Bacteroidetes, Proteobacteria, Spirochaetota, Deinococcota, Myxococcota and Verrucomicrobiot showed reduced abundance. CS@Se treatment primarily affected the abundance of Firmicutes, Actinobacteriota, Bacteroidetes, Proteobacteria, Desulfobacterota, Cyanobacteria and Deinococcota, leading to a profile similar to that of the control group.

The vertical axis represented sample information, while the horizontal axis represented species annotation information. The clustering tree on the left indicated species clustering, while the upper cluster tree showed clustering between sample groups. The heat map in the middle displayed the normalized values of the relative abundance of species for each row. The color scale indicated that the redder the color, the higher the abundance of the flora, while the bluer the color, the lower the abundance of the flora.

4. Conclusions

This study employed behavioral tests, pathological sections and 16S rDNA sequencing technology to investigate the potential mechanism of CS@Se in treating AD. The findings revealed that high dose of CS@Se (200 mg/kg·d) effectively improved learning and cognitive behavior in AD mice induced by D-gal and $AlCl_3$, alleviated anxiety, reduced pyramidal cell contraction and rupture in the CA3 and DG regions of the hippocampus, mitigated abnormal changes in synapses and mitochondria in hippocampal neurons, enhanced the richness and diversity of the intestinal flora, and increased the relative abundances of Firmicutes and Actinobacteria while decreasing the relative abundances of Bacteroidetes and Proteobacteria. Collectively, these results suggest that the intervention of CS@Se in AD involves multiple pathways and targets, but given the complex structure and composition of the intestinal flora, further exploration using multi-omics technology is necessary to elucidate the detailed mechanisms underlying the effects of CS@Se on the intestinal flora.

5. Discussion

The gut microbiota plays a crucial role in maintaining homeostasis within the body. Increasing evidence suggests a correlation between gut microbial dysbiosis and the progression of AD, although the exact mechanisms remain unclear. The gut microbiota may participate in the onset and progression of AD through four pathways [36]. Firstly, dysbiosis of the gut microbiota alters intestinal permeability, leading to bacterial translocation and the entry of gut-derived metabolites into the circulatory system, thereby triggering systemic inflammatory responses. Prolonged chronic inflammation exacerbates dysregulation of gut microbiota homeostasis, alters blood-brain barrier permeability, and induces or exacerbates central inflammatory environments, affecting neuronal connectivity networks and function. Secondly, the gut microbiota influences synaptic function and neurodevelopment processes through the release of neurotransmitters, further affecting neural network connectivity and brain regulatory functions. Thirdly, dysbiosis of the gut microbiota may continuously exacerbate brain Aβ deposition and brain tissue oxidative stress responses by activating brain inflammation signaling pathways. Finally, gut microbiota imbalance may upregulate the secretion of inflammatory factors and increase peripheral immune cell infiltration into the brain, affecting neuroinflammatory status.

Therefore, we studied the changes in the gut microbiota of AD mice and the effects of CS@Se on the gut microbiota of AD mice using mouse colon contents as samples. The study found that CS@Se could improve the diversity and richness of the gut microbiota in AD mice, increase the relative abundance of beneficial bacteria, and decrease the relative abundance of harmful bacteria. Moreover, differential microbial communities were observed at the phylum, class, order, and family levels. Clinical studies have found that compared to cognitively normal individuals, the relative abundance of Firmicutes and Actinobacteriota in the gut of AD patients significantly decreases, while the relative abundance of Bacteroidetes significantly increases [37]. These findings are consistent with our research results. Therefore, we used this as a starting point to explore the mechanisms and pathways of CS@Se in the treatment of AD from the perspective of gut microbiota.

As an important component of the gut microbiota, the Firmicutes phylum plays a role in fermenting indigestible carbohydrates and producing metabolites that promote health [38]. Within the Firmicutes phylum, the Clostridia class produce indole propionic acid, which inhibits endotoxemia and exhibits neuroprotective effects [39]. Lactobacillus, as one of the beneficial microbial groups within the Firmicutes phylum, inhibits pathogens and maintains intestinal microbial balance. Supplementation with Lactobacillus as a

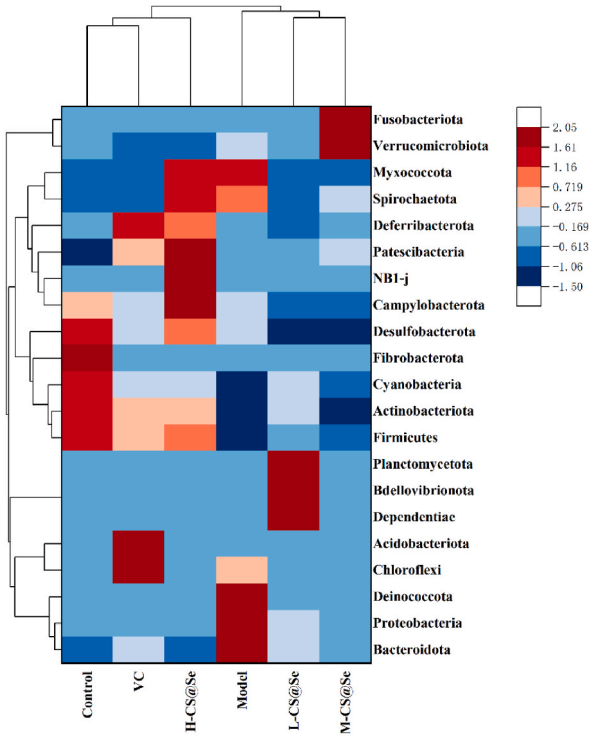

Fig. 9. Clustering of species abundance of flora in colon contents at phylum level.

probiotic has been shown to significantly improve cognitive function in AD patients [40]. In this study, compared to the control group, the relative abundance of Firmicutes phylum, Clostridia class, and Lactobacillus order in the colon contents of mice in the model group showed a significant decrease. In the CS@Se group, the relative abundance of these microbial groups was effectively restored, indicating that CS@Se could ameliorate the dysbiosis of the gut microbiota in AD mice. However, due to the vast and complex nature of the Firmicutes phylum, it also contains bacterial genera that may be harmful to health. Therefore, when using Firmicutes as a supplement for treatment, it is essential to carefully select specific genera and species.

The role of the phylum Bacteroidetes in the human body exhibits complex characteristics. For instance, within the Bacteroides genus, under normal conditions, it plays a role in regulating the immune system, maintaining intestinal barrier integrity, and preventing pathogen colonization. However, when it becomes dysbiotic, it may interfere with intestinal barrier function and trigger immune system dysregulation [41]. Studies have found that during old age, the gut microbiota exhibits a higher abundance of Bacteroidetes or lower uniqueness [42]. In this study, species clustering analysis at the phylum level showed that the gut microbiota of mice in the model group exhibited a higher clustering of the Bacteroidetes phylum. Additionally, in the clustering analysis at the sample level, they were farthest from the control group. This indicates significant differences in the gut microbiota of AD mice compared to the control group at the phylum level, suggesting an imbalance in the gut microbiota.

Helicobacteraceae belongs to the phylum Proteobacteria. *Helicobacter pylori* is present in the stomachs of more than half of the world's population. It not only triggers inflammatory markers, leading to gastrointestinal inflammation, but is also associated with various neurological complications such as stroke and AD [43,44]. As early as 2009, it was reported that the levels of *Helicobacter pylori* IgG in the cerebrospinal fluid and serum of AD patients were higher than those of cognitively normal age-matched individuals [45]. Previous studies have found that *Helicobacter pylori* filtrate increases Aβ by upregulating metalloproteinase-2 and damages synapses, thereby affecting spatial learning and memory in rats [46]. Uberti AF [47] pointed out that there was an association between *Helicobacter pylori* infection and AD, possibly mediated by its urease. In this experiment, the relative abundance of Helicobacteraceae was significantly increased in the model group mice, suggesting that after the onset of AD, there was an upregulation of Helicobacteraceae expression, leading to an inflammatory response in the body, while the regulatory effect of CS@Se reduces the relative abundance of Helicobacteraceae.

Collectively, these results suggest that the intervention of CS@Se in AD involves multiple pathways and targets, but given the complex structure and composition of the intestinal flora, further exploration using multi-omics technology is necessary to elucidate the detailed mechanisms underlying the effects of CS@Se on the intestinal flora.

Ethics approval

All animal experiments were conducted in accordance with the guidelines set by the Institutional Animal Ethics Committee and

were approved by the Experimental Animal Ethics Committee of Shandong First Medical University (No.: W202302200002).

Fundings

This work was supported by Natural Science Foundation of Shandong Province (No. ZR2020MH410), Shandong First Medical University (Shandong Academy of Medical Sciences) SRTP (No. 2022104391637) and Innovation and Entrepreneurship Training Program for College Students in Shandong Province (No. S202310439038).

Data availability statement

Data will be made available on request.

CRediT authorship contribution statement

Changfang Fu: Writing – original draft, Methodology, Data curation. **Xinyue Wang:** Supervision, Methodology, Data curation. **Wei Zhou:** Methodology, Investigation, Data curation. **Qi Gao:** Supervision, Investigation, Conceptualization. **Junjun Luo:** Methodology, Investigation. **Yuqin Li:** Writing – review & editing, Methodology, Investigation, Funding acquisition.

Declaration of competing interest

The authors declare that they have no known competing financial interests or personal relationships that could have appeared to influence the work reported in this paper.

References

[1] I. Kolaj, S.I. Liyanage, D.F. Weaver, Phenylpropanoids and Alzheimer's disease: a potential therapeutic platform, Neurochem. Int. 120 (2018) 99–111.
[2] Q. Wang, Y. Hao, Y. Yang, et al., A Chinese pedigree with early-onset familial Alzheimer's disease caused by presenilin 1 p.G378E mutation, Chin. J. Neurol. 50 (2017) 208–212.
[3] R.L. Frozza, M.V. Lourenco, F.G. De Felice, Challenges for Alzheimer's disease therapy: insights from novel mechanisms beyond memory defects, Front. Neurosci. 12 (2018) 37.
[4] A.A. Rostagno, Pathogenesis of Alzheimer's disease, Int. J. Mol. Sci. 24 (2022) 107.
[5] S. Tiwari, V. Atluri, A. Kaushik, et al., Alzheimer's disease: pathogenesis, diagnostics, and therapeutics, Int. J. Nanomedicine. 14 (2019) 5541–5554.
[6] H. Geng, S. Li, J. Yin, et al., Coping with the challenge of aging and strengthening the research on the prevention and control of Alzheimer's disease, J. Chongqing Med. Univ. 44 (2019) 386–388.
[7] Y. Sun, C. Yan, L. He, et al., Inhibition of ferroptosis through regulating neuronal calcium homeostasis: an emerging therapeutic target for Alzheimer's disease, Ageing Res. Rev. 87 (2023) 101899.
[8] D.S. Knopman, D.T. Jones, M.D. Greicius, Failure to demonstrate efficacy of aducanumab: an analysis of the EMERGE and ENGAGE trials as reported by Biogen, December 2019, Alzheimers Dement 17 (2021) 696–701.
[9] E. McDade, I. Voytyuk, P. Aisen, et al., The case for low-level BACE1 inhibition for the prevention of Alzheimer disease, Nat. Rev. Neurol. 17 (2021) 703–714.
[10] F.E. Artuzi, E. Puricelli, C.E. Baraldi, et al., Reduction of osteoarthritis severity in the temporomandibular joint of rabbits treated with chondroitin sulfate and glucosamine, PLoS One 15 (2020) e0231734.
[11] K. Imada, H. Oka, D. Kawasaki, et al., Anti-arthritic action mechanisms of natural chondroitin sulfate in human articular chondrocytes and synovial fibroblasts, Biol. Pharm. Bull. 33 (2010) 410–414.
[12] L.H.C. Medeiros, B.M.F. Vasconcelos, M.B. Silva, et al., Chondroitin sulfate from fish waste exhibits strong intracellular antioxidant potential, Braz. J. Med. Biol. Res. 54 (2021) e10730.
[13] R. Lan, Y. Li, R. Shen, et al., Preparation of low-molecular-weight chondroitin sulfates by complex enzyme hydrolysis and their antioxidant activities, Carbohydr. Polym. 241 (2020) 116302.
[14] L. Yan, D. Wang, Y. Yu, et al., Fucosylated chondroitin sulfate 9-18 oligomers exhibit molecular size-independent antithrombotic activity while circulating in the blood, ACS Chem. Biol. 15 (2020) 2232–2246.
[15] P. Melgar-Lesmes, A. Sánchez-Herrero, F. Lozano-Juan, et al., Chondroitin sulphate attenuates atherosclerosis in ApoE knockout mice involving cellular regulation of the inflammatory response, Thromb. Haemost. 118 (2018) 1329–1339.
[16] S. Song, H. Peng, Q. Wang, et al., Inhibitory activities of marine sulfated polysaccharides against SARS-CoV-2, Food Funct. 11 (2020) 7415–7420.
[17] S. Morla, Glycosaminoglycans and glycosaminoglycan mimetics in cancer and inflammation, Int. J. Mol. Sci. 20 (2019) 1963.
[18] F. He, D. Yang, Q. Zhu, Advances in research into the effect of chondroitin sulfate proteoglycan on orderly regeneration of peripheral nerves, Chinese Journal of Orthopaedic Trauma 21 (2019) 1097–1100.
[19] D. Nowicka, A. Gręda, Chondroitin sulfate metabolism in the brain, Acta Neurobiol. Exp. 79 (2019) 338–351.
[20] Q. Zhang, J. Li, C. Liu, et al., Protective effects of low molecular weight chondroitin sulfate on amyloid beta (Aβ)-induced damage in vitro and in vivo, Neuroscience 305 (2015) 169–182.
[21] X. Qin, K. Nong, Q. Lv, et al., Research progress of the antioxidant effects of trace element selenium, China Food Additives 33 (2022) 272–278.
[22] Y.S. Qiu, L. Shao, D.J. Chen, et al., Research progress on anti-tumor effect of selenium, World ClinicaI Drug 38 (2017) 344–347.
[23] J. Xu, Y. Gong, Y. Sun, et al., Impact of selenium deficiency on inflammation, oxidative stress, and phagocytosis in mouse macrophages, Biol. Trace Elem. Res. 194 (2020) 237–243.
[24] M. Kiełczykowska, J. Kocot, M. Paździor, Selenium - a fascinating antioxidant of protective properties, Adv. Clin. Exp. Med. 27 (2018) 245–255.
[25] F. Gao, J. Zhao, P. Liu, et al., Preparation and in vitro evaluation of multi-target-directed selenium-chondroitin sulfate nanoparticles in protecting against the Alzheimer's disease, Int. J. Biol. Macromol. 142 (2020) 265–276.
[26] H.R. Bulgart, E.W. Neczypor, L.E. Wold, et al., Microbial involvement in Alzheimer disease development and progression, Mol. Neurodegener. 15 (2020) 42.
[27] B. Sun, T. Chen, T. Wang, et al., Interaction between gut microbiota and brain-gut axis: research progress, Chin. J. Microecol. 28 (2016) 1206–1211.
[28] T.J. Li, D.X. Jia, Y. Zhao, et al., Gut microbiota and Alzheimer's disease, Journal of International Pharmaceutical Research 43 (2016) 15–19+32.
[29] M. Minemura, Y. Shimizu, Gut microbiota and liver diseases, World J. Gastroenterol. 21 (2015) 1691–1702.
[30] P. Cieślik, M. Borska, J.M. Wierońska, A comparative study of the impact of NO-related agents on MK-801- or scopolamine-induced cognitive impairments in the Morris water maze, Brain Sci. 13 (2023) 410.
[31] F.U. Amin, S.A. Shah, M.O. Kim, Vanillic acid attenuates $A\beta_{1-42}$-induced oxidative stress and cognitive impairment in mice, Sci. Rep. 7 (2017) 40753.

[32] M. Wan, S. Sun, X. Di, et al., Icariin improves learning and memory function in Aβ1-42-induced AD mice through regulation of the BDNF-TrκB signaling pathway, J. Ethnopharmacol. 318 (2023) 117029.
[33] E.A.K. Prieur, N.M. Jadavji, Assessing spatial working memory using the spontaneous alternation Y-maze test in aged male mice, Bio Protoc 9 (2019) e3162.
[34] J.S. Jung, J.J. Yan, H.M. Li, et al., Protective effects of a dimeric derivative of ferulic acid in animal models of Alzheimer's disease, Eur. J. Pharmacol. 782 (2016) 30–34.
[35] M. Saadullah, M. Fakhar-e-Alam, S. Muzammil, et al., Evaluation of molecular mechanisms responsible for in vivo anti-Alzheimer's property of Euphorbia cotinifolia methanol extract, J. King Saud Univ. Sci. 35 (2023) 102785.
[36] L. Zhang, Z.F. Fan, Z.P. Zhang, et al., Research progress on pathogenesis and therapeutic drugs of Alzheimer's disease, Chin. J. Med. Chem. 31 (6) (2021) 438–446+469.
[37] N. M Vogt, R.L. Kerby, K.A. Dill-McFarland, et al., Gut microbiome alterations in Alzheimer's disease, Sci. Rep. 7 (1) (2017) 13537.
[38] Y. Huang, X. Shi, Z. Li, et al., Possible association of Firmicutes in the gut microbiota of patients with major depressive disorder, Neuropsychiatr Dis Treat 14 (2018) 3329–3337.
[39] E.R. Murray, M. Kemp, T.T. Nguyen, The microbiota-gut-brain Axis in Alzheimer's disease: a review of taxonomic alterations and potential avenues for interventions, Arch. Clin. Neuropsychol. 37 (3) (2022) 595–607.
[40] E. Akbari, Z. Asemi, R. Daneshvar Kakhaki, et al., Effect of probiotic supplementation on cognitive function and metabolic status in Alzheimer's disease: a randomized, double-blind and controlled trial, Front. Aging Neurosci. 8 (2016) 256.
[41] W.J. Lukiw, The microbiome, microbial-generated proinflammatory neurotoxins, and Alzheimer's disease, J Sport Health Sci 5 (4) (2016) 393–396.
[42] T. Wilmanski, C. Diener, N. Rappaport, et al., Gut microbiome pattern reflects healthy ageing and predicts survival in humans, Nat. Metab. 3 (2) (2021) 274–286.
[43] J. Kountouras, F. Tsolaki, M. Tsolaki, et al., Helicobacter pylori-related ApoE 4 polymorphism may be associated with dysphagic symptoms in older adults, Dis. Esophagus 29 (7) (2016) 842.
[44] A.G. Gravina, R.M. Zagari, C. De Musis, et al., Helicobacter pylori and extragastric diseases: a review, World J. Gastroenterol. 24 (29) (2018) 3204–3221.
[45] J. Kountouras, M. Boziki, E. Gavalas, et al., Increased cerebrospinal fluid Helicobacter pylori antibody in Alzheimer's disease, Int. J. Neurosci. 119 (6) (2009) 765–777.
[46] X.L. Wang, J. Zeng, J. Feng, et al., Helicobacter pylori filtrate impairs spatial learning and memory in rats and increases β-amyloid by enhancing expression of presenilin-2, Front. Aging Neurosci. 6 (2014) 66.
[47] A.F. Uberti, N. Callai-Silva, M.V.C. Grahl, et al., Helicobacter pylori urease: potential contributions to Alzheimer's disease, Int. J. Mol. Sci. 23 (6) (2022) 3091.